VDMA
Fluid Power Association

23rd ISC

International Sealing Conference

Stuttgart, Germany
Sept.30 - Oct.1, 2026

Sealing the future –
Facing the challenges of tomorrow

IMA
UNI STUTTGART

Fachverband Fluidtechnik im VDMA e. V. Lyoner Str. 18
50628 Frankfurt am Main
Germany

Phone +49 69 6603-1513
E-Mail maximilian.baxmann@vdma.eu

Internet www.vdma.eu/fluid

Numerical Investigation of Leakage in Injectors for Novel Gaseous Fuels Considering Surface Topography

Marius Hofmeister, Anmol Kasera, Georg Michael Puntigam, Felix Justin Fischer, Katharina Schmitz

The sealing performance of injector seat valves in combustion engines is critically affected by microscopic leakage paths formed by surface roughness and elastic deformation of the contacting bodies. With the introduction of gaseous fuels such as H_2 and NH_3, leakage mechanisms are increasingly governed by micro- and nanoscale gap geometries, where the characteristic dimensions approach the molecular size of the fluid. In contrast to conventional gaseous fuels such as LPG or CNG, these fuels are considered for application in diesel-type high-pressure injection systems, leading to substantially increased requirements regarding injector sealing, contact mechanics, and allowable leakage. In this study, a numerical simulation framework for leakage prediction in seat valves is extended to investigate sealing behaviour under gaseous fuel conditions. The model is based on a modified Hagen–Poiseuille law formulation combined with an effective gap approach to represent the interconnected network of micro-channels within the sealing interface. The real contact area and pressure-dependent gap distribution are obtained using Persson's contact mechanics, accounting for elasto-plastic deformation of surface asperities across multiple length scales. A particular focus is placed on the influence of surface roughness power spectra, seat geometry, and contact pressure on the resulting leakage paths. Numerical studies are conducted to quantify how variations in roughness amplitude, wavelength content, and macroscopic geometry affect leakage rates and required sealing forces. The study highlights the limitations of conventional sealing design criteria when applied to gaseous fuels and identifies key geometric and surface-related parameters governing tightness. The findings support the numerical design and optimization of injector seat valves for future applications involving gaseous alternative fuels.

1 Introduction

Alternative gaseous energy carriers such as ammonia and hydrogen are gaining increasing attention, as they offer several advantages over conventional fossil fuels and even carbon-based bio-hybrid fuels. While bio-hybrid fuels enable a closed carbon cycle, they still lead to local emissions during combustion. In contrast, ammonia and hydrogen can be utilized without direct CO_2 emissions at the point of use. [1]

In addition to their application in fuel cells, ammonia in particular is considered a promising fuel for internal combustion engines due to its significantly higher volumetric energy density compared to gaseous hydrogen [2]. Consequently, first experimental studies have demonstrated the feasibility of operating both compression-ignition and spark-ignition engines with ammonia. Furthermore, high efficiencies comparable to conventional combustion concepts have been reported in recent investigations. [3] The term gaseous refers to fuels in their standard ambient state, although their phase may differ under the high-pressure and high-temperature conditions prevailing during injection.

The use of ammonia and hydrogen in internal combustion engines is associated with several challenges. Ammonia exhibits low reactivity and high ignition delay, which can result in incomplete combustion and increased emissions of unburned species [4]. In addition, its energy density remains lower than that of diesel fuel, and its toxicity imposes strict requirements on handling and system design. Moreover, both ammonia and hydrogen differ significantly from conventional fuels in terms of thermophysical properties, including boiling point, molecular size, and transport properties. [5]

These differences directly affect flow behaviour and sealing performance in fuel injection systems. In particular, leakage phenomena in injectors are expected to differ substantially from those observed with diesel or methanol due to low viscosity of ammonia and hydrogen [5]. Leakage at the injector nozzle seat can lead to uncontrolled fuel release into the combustion chamber, commonly referred to as dribble. This results in a range of detrimental effects, including increased emissions, thermal overloading of engine components, oil dilution, reduced efficiency, and combustion instabilities. [6]

Given the critical importance of leakage and the expectation that it may be more pronounced for ammonia and hydrogen, a detailed understanding of the interplay between surface properties, contact pressure, fluid properties, and material behaviour is essential. However, the scope of this study is limited to a comparative analysis of ammonia, diesel, and methanol.

In this work, leakage is investigated using a simulation framework that combines the contact mechanics model developed by Bo Persson [7], [8] with a flow model based on the Hagen–Poiseuille equation. The latter is introduced in the first part of the paper, together with its underlying modelling approach and relevant prior developments. [9]

To account for the strong influence of fluid properties, the fuels considered and their corresponding fluid models are described in detail, including their dependence on temperature and pressure. In particular, the properties viscosity, density, and boiling point are taken into account. In addition, representative surface characteristics typical of diesel injector components are analyzed and incorporated into the study. Subsequently, leakage rates are computed for varying surface conditions and compared across different fuels.

2 Injector sealing system

In **Figure 1** the schematic sketch of a state-of-the-art injector sealing system is shown. The sealing system typically consists of a conical needle that interfaces with a matching conical seat to ensure reliable closure under high-pressure conditions in the closed state. However, leakage can still occur even in the closed state, as the interacting surfaces are not ideally smooth. This leads to the formation of microchannels that connect the high-pressure region with the combustion chamber. As already mentioned, leakage at the injector nozzle seat can lead to uncontrolled fuel release into the combustion chamber, commonly referred to as dribble. This results in a range of detrimental effects, including increased emissions, thermal overloading of engine components, oil dilution, reduced efficiency, and combustion instabilities. [6]

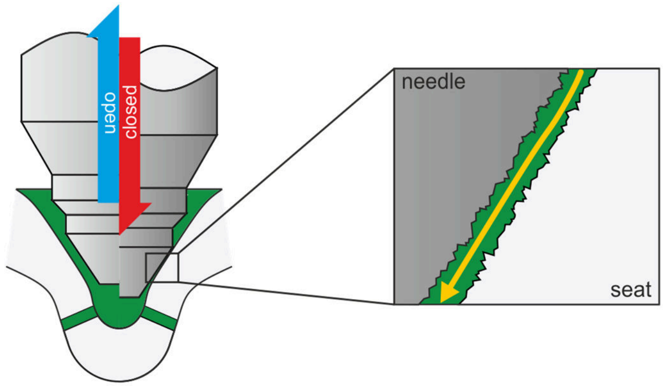

Figure 1: State of the art injector sealing system

Typical cone angles used in diesel injector needle–seat systems lie in the range of approximately 30°–45° (half-angle α), corresponding to included angles of about 60°–90°, depending on injector design and spray targeting requirements. The corresponding seat diameters typically range from 1 to 2 mm [10], [11]. Injector needle seating forces are generally on the order of several hundred Newtons, resulting from the combined effect of hydraulic pressure and spring preload. For modern common-rail systems, representative values range from approximately 100 N to 800 N. A slight angular mismatch between the needle and seat ($\Delta\alpha = 0.2° \dots 0.5°$), in combination with these high contact forces, leads to the formation of a narrow line contact characterized by high local contact pressures and excellent sealing performance [10].

Both the needle and the seat are commonly manufactured from hardened alloy steels, frequently combined with wear-resistant materials such as tungsten carbide at the needle tip to improve durability. To minimize leakage into the combustion chamber, the contacting surfaces are produced using precision grinding followed by lapping, enabling excellent form accuracy and ultra-low surface roughness. Modern injector sealing interfaces typically exhibit surface roughness values in the range of $R_a \approx 0.02 - 0.05\ \mu\text{m}$, whereas functional sealing performance can still be maintained up to approximately $R_a \approx 0.6\ \mu\text{m}$. [10], [12], [13], [14]

While conventional amplitude parameters such as the arithmetic mean roughness Ra are commonly used to characterize injector sealing surfaces, they are not sufficient to fully describe the functional behaviour of the needle–seat contact. In particular, leakage through the sealing interface is governed by the distribution of roughness across different length scales, which can be captured by the surface roughness power spectral density (PSD) [7]. The PSD $C(q)$, defined as the Fourier transform of the height–height correlation function, describes how surface roughness is distributed over spatial frequencies (wave numbers q). For precision-ground and lapped steel surfaces typically used in injector applications, the PSD exhibits self-affine behaviour over a wide range of scales and can be approximated by a power law of the form given in Equation (1), where H is the Hurst exponent.

$$C(q) \sim q^{-2(1+H)} \tag{1}$$

For injector-grade sealing surfaces, typical values lie in the range of $H \approx 0.7$ to 0.85, indicating relatively smooth surfaces with reduced high-frequency roughness components.

The relevant wave number range for injector sealing contacts can be estimated based on typical surface characteristics of precision-lapped metallic interfaces. These surfaces, which are commonly used in injector needle–seat systems, exhibit roughness spectra spanning approximately from $q \approx 10^4$ m^{-1} to $q \approx 10^8$ m^{-1}, corresponding to wavelength scales from the sub-millimeter down to the nanometer range. Within this interval, the power spectral density typically decreases from about $C(q) \approx 10^{-13}\ \mathrm{m}^3$ at low wave numbers to approximately $10^{-20}\ \mathrm{m}^3$ at high wave numbers for high-quality lapped surfaces with roughness values of $R_a \approx 0.02\text{–}0.05\ \mu\mathrm{m}$ [15], [16].

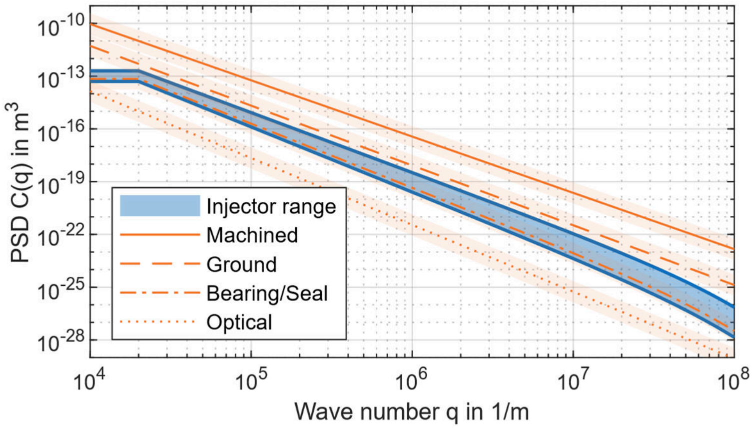

Figure 2: Comparison of power spectral densities (PSD) for different classes of technical surfaces. The blue-shaded region represents the typical range for injector needle–seat sealing surfaces.

For technical surfaces, characteristic regimes can be identified: a low-frequency plateau associated with form deviations and waviness, a self-affine regime governed by power-law decay, and a high-frequency cutoff determined by the manufacturing process. A schematic representation of typical PSD curves is shown in **Figure 2**. Based on reported values of the Hurst exponent H and the approximately constant power spectral density at low frequencies ($C(q) \approx \mathrm{const.}$), an envelope for injector surfaces can be constructed that bounds the range of possible PSD curves.

3 Simulation model

The simulation framework employed in this study builds upon a combination of the contact mechanics approach introduced by Persson [7] and a leakage model derived from the Hagen–Poiseuille equation. While the methodology for leakage in ball-seat valves has been described in detail in previous studies [17], a concise summary of its adaptation to the geometry of automotive injector applications is provided here.

The modelling approach comprises three coupled levels: a macroscopic analysis of the contact mechanics, a microscopic description of the leakage paths, and the subsequent calculation of the leakage flow. The surface properties described above and the fluid properties introduced below serve as input parameters. An overview of the simulation framework is shown in **Figure 3**. The individual components are described in the following.

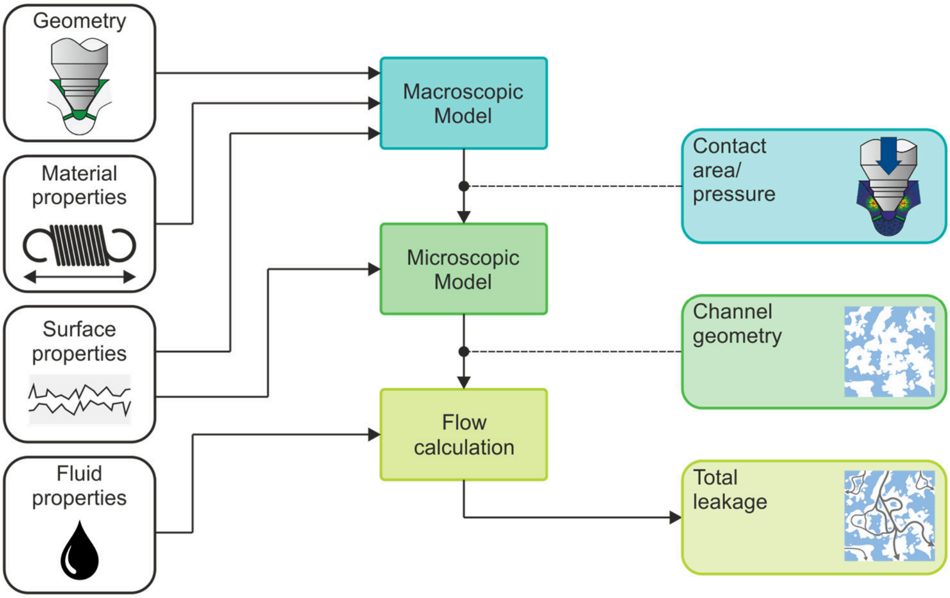

Figure 3: Overview of simulation framework for determining leakage

3.1 Macroscopic model

At the macroscopic level, the objective is to determine the contact pressure distribution at the interface between the conical needle and seat elements. This is achieved using an analytical representation of the contacting geometries together with the elastic material properties of both bodies.

A key aspect of this analysis is the consideration of surface roughness. As mentioned beforehand real surfaces exhibit multi-scale roughness, which alters the nominal contact by effectively broadening the contact zone, increasing the real contact area, and reducing peak pressures. These effects are commonly incorporated through a contact–pressure relationship linking local surface separation to contact pressure.

Several approaches exist to establish this relationship, such as the classical Greenwood–Williamson model [18]. In the present work, the formulation proposed by Persson is adopted, as it allows for a consistent treatment of roughness across multiple length scales using a spectral description. In addition, this framework can account for plastic deformation of asperities, which further influences the effective sealing behaviour.

The resulting contact pressure distribution serves as the primary input for the subsequent microscopic analysis.

3.2 Microscopic model

The microscopic model resolves the leakage mechanism by describing the flow through a network of interconnected micro-channels that form within the apparent contact area. Based on the macroscopic pressure distribution, an effective contact width is defined, which provides a characteristic length scale for the leakage path. The channel height is then determined using a Persson-based approach that relates local pressure to interfacial separation [7].

To identify continuous flow paths, concepts from percolation theory are employed. This allows the determination of a critical channel network spanning the contact region, representing the dominant leakage pathway through the interface. The geometric properties of this path—such as its characteristic width, length, and its relation to the macroscopic contact circumference—are used to define an equivalent leakage slit for the subsequent flow calculation.

3.3 Fluid properties and flow calculation

The volumetric/gravimetric flow rate through this gap is finally calculated using the Hagen–Poiseuille equation for viscous flow in narrow rectangular channels. Given the very high injection pressures typical of diesel combustion engines, which ranges from several hundred to a few thousand bars, the injected fuels are expected to remain in a single-phase liquid state throughout the leakage gap. [6] The Hagen–Poiseuille equation is therefore applied under this single-phase liquid assumption for all three fuels considered. Diesel and methanol are treated as liquids under all investigated conditions, while ammonia, although gaseous at ambient conditions, is treated as a pressurized liquid under the injection pressures and temperatures examined here.

$$\dot{V} = \frac{h^3 B}{12\eta}\frac{\partial p}{\partial x} \Leftrightarrow \dot{m} = \frac{\rho h^3 B}{12\eta}\frac{\partial p}{\partial x} \qquad (2)$$

The fluid properties required for the leakage calculation, namely viscosity and density, are presented in **Figure 4**. The corresponding data for diesel are obtained from literature and are based on a model introduced by Drumm [5]. For methanol and ammonia, the viscosity and density correlations were derived from regression analyses performed on thermophysical property data generated using CoolProp [19]. These properties were calculated for the fuels in liquid phase under the investigated conditions.

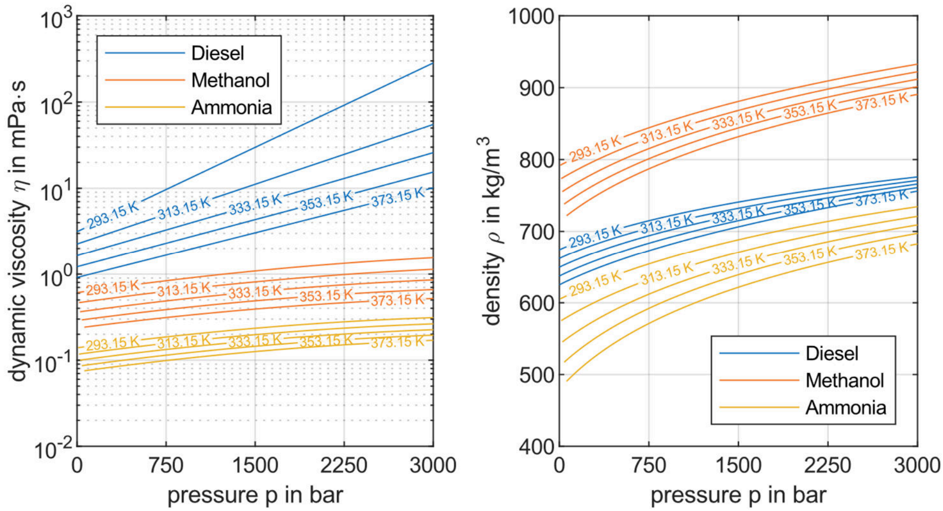

Figure 4: Fluid properties (viscosity left, density right) of different fuels in liquid state

According to the fluid mechanical properties presented in Figure 4, significant differences can be observed between the investigated fluids. Methanol and especially ammonia exhibit substantially lower viscosities, which are approximately one to two orders of magnitude lower than that of diesel fuel. Furthermore, a strong influence of pressure and temperature on the viscosity is visible. As the pressure gradient is high, its influence on the leakage cannot be neglected. For this reason, the Hagen-Poiseuille equation from (2) is rearranged as shown in (3) and subsequently solved numerically for the gaps obtained from the microscopic model.

$$\dot{m} = \frac{h^3 B}{12L} \int_{p_{out}}^{p_{in}} \frac{\rho(p_f, T)}{\eta(p_f, T)} dp_f \tag{3}$$

Besides the strong influence of pressure on viscosity and density, both properties also depend on fluid temperature. To estimate the temperature rise within the sealing gap due to viscous dissipation and its potential impact on leakage, the Péclet number given in Equation (4) can be considered.

$$Pe = \frac{hv\rho c_p}{\lambda} \tag{4}$$

The Péclet number represents the ratio of advective to diffusive heat transport and depends on the thermophysical properties heat capacity c_p, thermal conductivity λ, and density ρ, as well as on the characteristic length scale of the flow channel, namely the channel height h , and the characteristic flow velocity v. For small Péclet numbers ($Pe \ll 1$), diffusive heat conduction dominates, resulting in nearly isothermal conditions. In injector sealing gaps, the characteristic gap heights h are typically in the sub-micrometer range, leading to low flow velocities v. Consequently, the Péclet number is expected to be well below unity, indicating that heat is efficiently dissipated. Therefore, in the present study, temperature increases due to viscous dissipation are neglected.

The continuum assumption was assessed using the Knudsen number,

$$Kn = \frac{\Lambda}{h} \tag{5}$$

For liquid and dense-fluid conditions, the molecular mean free path, Λ, is of the order of the molecular diameter, approximately $10^{-10}\ \mathrm{m}$. Consequently, for effective gap heights of $h \approx 10^{-8}\ \mathrm{m}$ (derived later in section 4), Kn is of the order of 10^{-2}, indicating that the continuum approximation remains a reasonable first-order assumption. However, for the smallest calculated gaps approaching $h \approx 10^{-9}\ \mathrm{m}$, rarefaction, slip, molecular layering, and surface-interaction effects may become relevant. Therefore, the corresponding leakage values should be interpreted as continuum-based estimates. [20]

4 Results and discussion

In this study the four injectors listed in **Table 1** are investigated with respect to leakage behavior. While identical diameters and mechanical properties (E, ν) were used for all injectors, the half cone angle α and the surface parameters (H, R_a) were varied.

Table 1: Injector parameters

	Injector 1	**Injector 2**	**Injector 3**	**Injector 4**
d	2 mm			
α	30°	45°	30°	45°
$\Delta\alpha$	0.2°			
H	0.7		0.85	
R_a	0.05		0.02	
q_0	2e4 1/m			
E	210 GPa			
ν	0.3			

For the four injectors, the effective gap height h_{eff}, which is the key parameter for the leakage calculation, was first investigated as a function of the injector force F. The corresponding results are shown in **Figure 5** .

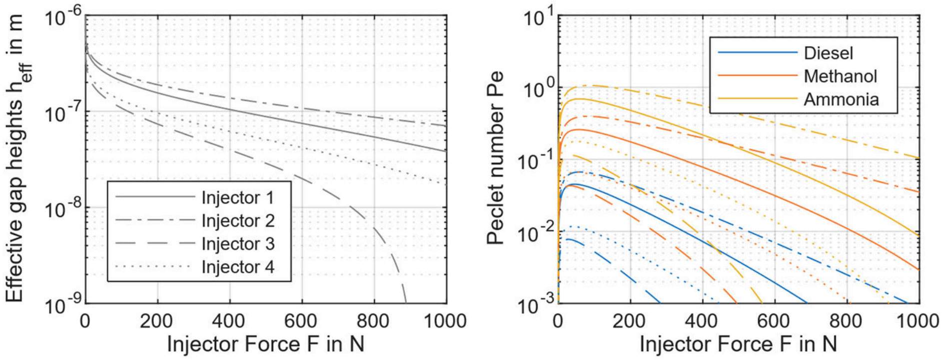

Figure 5: Effective gap height h_{eff} and resulting Pe numbers at 333.15K

For contact forces approaching zero, the gap between the injector and the seat remains fully open. Consequently, the effective gap height tends toward infinity. With increasing contact force, the gap progressively closes until complete closure occurs at high pressure levels, which can be observed from the steep decrease in gap height for Injector 3. In the relevant force range around 800 N, the effective gap height lies between $10^{-6}$and 10^{-7} m, depending on the injector configuration.

Based on the effective gap height, the Péclet number Pe was calculated in a subsequent step using Equation (4). It was assumed that the differential fluid pressure is proportional to the contact force F and can be determined according to Equation (6).

$$p_f \approx \frac{F}{A_{eff}} \approx \frac{4F}{\pi d^2} \tag{6}$$

The resulting Péclet numbers are primarily in the range of $Pe \approx 1$ for low pressure levels. With increasing contact force, the Péclet number decreases and becomes significantly smaller than 1 for all injectors and fluids in the relevant force range around 800 N. This justifies the assumption made in section 3 that no significant heating of the fluid occurs.

The calculated leakage rates for the four injectors and the fuels diesel, methanol, and ammonia are shown in Fehler! Verweisquelle konnte nicht gefunden werden.. The arrows indicate an increase in temperature from 293.15 K to 373.15 K in steps of 20 K. It can be observed that the leakage strongly depends on the applied injector geometry and surface characteristics, but even more significantly on the selected fuel. In particular, for low contact forces of approximately 100 N, the leakage rate of ammonia is about one order of magnitude higher than that of diesel under identical pressure and temperature conditions. This behavior can be attributed to the considerably higher viscosity of diesel fuel.

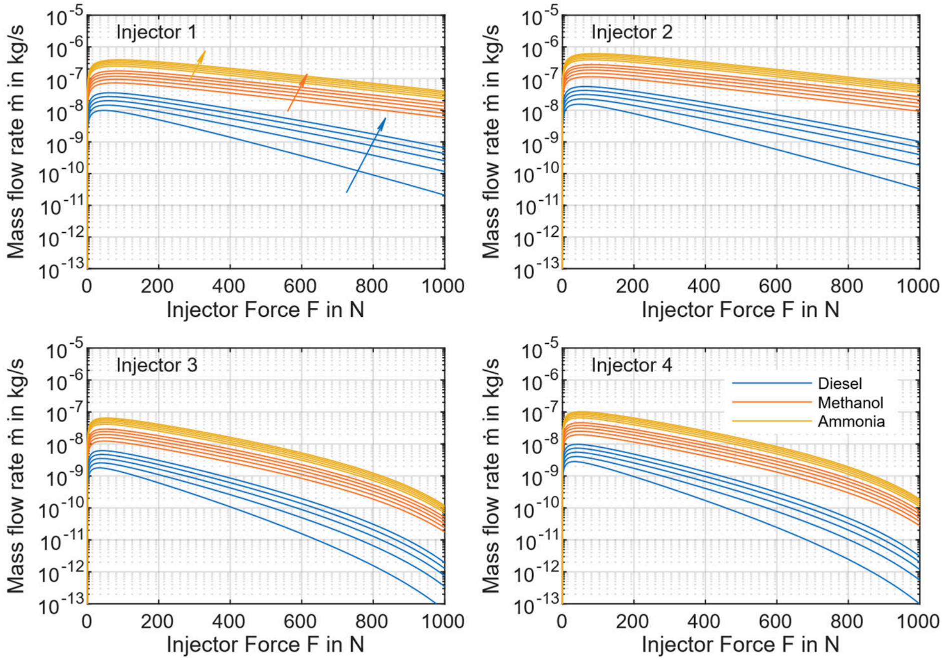

Figure 6: Leakage mass flow rate for Injector 1-4 for the investigated fuels and different temperatures (293.15 – 373.15 K)

Although the leakage decreases for all fuels with increasing pressure, the difference between diesel and the other two fuels becomes more pronounced. At the highest investigated contact force, the leakage rate of ammonia exceeds that of diesel by approximately two orders of magnitude. This behavior is mainly caused by the significantly stronger pressure–viscosity relationship of diesel fuel, which is clearly illustrated in Figure 4. According to Equation (3), this results in a substantially increased effective viscosity and an additional sealing effect at elevated pressures.

5 Summary and Conclusion

In this study, injector leakage for the fuels diesel, methanol, and ammonia was investigated using a simulation model based on theoretical surface data representative of lapped injector surfaces. The results demonstrated that ammonia leads to increased leakage due to its lower viscosity. In particular, the significantly weaker pressure–viscosity dependence of ammonia results in comparatively high leakage rates, especially under high contact forces and pressures. The simulation results indicate that the use of ammonia in diesel engines imposes increased requirements on injector surface quality, which become particularly relevant in high-pressure applications. The leakage predictions, especially at very small effective gap heights, should be interpreted with caution because molecular-scale effects may become relevant beyond the continuum regime. Future work should therefore extend the model accordingly. As this study considered only theoretical surface topographies, future work will also focus on the investigation of real injector surfaces and on the experimental validation of the presented results.

6 Acknowledgements

The Fuel Chemical Science Center (FSC2) is funded by the German Council of Science and Humanities (Wissenschaftsrat, WR) and by Deutsche Forschungsgemeinschaft (DFG).

7 Nomenclature

Variable	***Description***	***Unit***
α	Injector half angle	[°]
$\Delta\alpha$	Angle mismatch (seat/needle)	[°]
η	Dynamic viscosity	[Pa·s]
λ	Thermal conductivity	[W/(m·K)]
Λ	Mean Free Path	[m]
ν	Poisson's ratio	[-]
ρ	Density	[kg/m^3]
B	Flow channel width	[m]
d	Injector diameter	[m]
E	E-modulus	[GPa]
F	Injector force	[N]
H	Hurst coefficient	[-]
$h_{(eff)}$	(Effective) Gap heights	[m]
Kn	Knudsen Number	[-]
L	Flow channel length	[m]
Pe	Péclet number	[-]
PSD	Power spectral densities	[m^3]
p_f	Fluid Pressure	[Pa]
Q	Volumetric flow rate	[m^3/s]
q	Wavenumber	[1/m]
R_a	Arithmetic surface roughness	[µm]

8 References

[1] DEMIRBAS, Ayhan: *Biofuels securing the planet's future energy needs*. In: *Energy Conversion and Management* 50 (2009), Nr. 9, S. 2239–2249

[2] ZAMFIRESCU, C. ; DINCER, I.: *Using ammonia as a sustainable fuel*. In: *Journal of Power Sources* 185 (2008), Nr. 1, S. 459–465

[3] LI, Zhengling ; LÜCKERATH, Moritz ; PISCHINGER, Stefan ; BOBERIC, Aleksandar ; FRANZKE, Bjoern ; DHONGDE, Avnish ; JAGODZINSKI, Bartosch ; BURROWS, John ; KORKMAZ, Metin: Ammonia Combustion with Ignition Improvement Measures in a High-Speed Marine Application. In: *International Conference on Engines 2025, Capri, Italy*.

[4] NOLTE, Adrian ; NOÉ, Micha Renè ; HEUFER, Karl Alexander: *Laminar Burning Velocities at Engine-Relevant Conditions of Methane, Hydrogen, and Ammonia: A Rapid Compression Machine Study*. In: *Energy & Fuels* 38 (2024), Nr. 16, S. 15622–15629

[5] DRUMM, Sebastian Michael: *Entwicklung von Messmethoden hydraulischer Kraftstoffeigenschaften unter Hochdruck*. Zugl.: Aachen, Techn. Hochsch., Diss., 2012. Aachen : Shaker, 2012 (Reihe Fluidtechnik D 69)

[6] HEYWOOD, John B.: *Internal combustion engine fundamentals*. Second revised edition. New York, Chicago, San Francisco und 9 andere : McGraw-Hill Education, 2018 (McGraw-Hill series in mechanical engineering)

[7] PERSSON, B. N. J.: *Fluid dynamics at the interface between contacting elastic solids with randomly rough surfaces*. In: *Journal of physics. Condensed matter : an Institute of Physics journal* 22 (2010), Nr. 26, S. 265004

[8] PERSSON, B. N. J.: *Theory of rubber friction and contact mechanics*. In: *The Journal of Chemical Physics* 115 (2001), Nr. 8, S. 3840–3861

[9] FISCHER, Felix ; MURRENHOFF, Hubertus ; SCHMITZ, Katharina: *Influence of normal force in metallic sealing*. In: *Engineering Reports* 3 (2021), Nr. 10

[10] ROBERT BOSCH GMBH: *Blind hole injection nozzle for internal combustion engines*. Veröffentlichungsnr. DE19931761A1

[11] BAI, Y. ; FAN, L. Y. ; MA, X. Z. ; PENG, H. L. ; SONG, E. Z.: *Effect of injector parameters on the injection quantity of common rail injection system for diesel engines*. In: *International Journal of Automotive Technology* 17 (2016), Nr. 4, S. 567–579

[12] BERGSTRAND, Pär ; DENBRATT, Ingemar: The Effects of Multirow Nozzles on Diesel Combustion. In: *SAE 2003 World Congress & Exhibition*.

[13] MONIETA, Jan ; KASYK, Lech: *Optimization of Design and Technology of Injector Nozzles in Terms of Minimizing Energy Losses on Friction in Compression Ignition Engines*. In: *Applied Sciences* 11 (2021), Nr. 16, S. 7341

[14] MONTAJIR, Rahman M. ; TSUNEMOTO, H. ; ISHITANI, H. ; MINAMI, T.: Fuel Spray Behavior in a Small DI Diesel Engine: Effect of Combustion Chamber Geometry. In: *SAE 2000 World Congress, Detroit, Michigan, United States*.

[15] STACHOWIAK, Gwidon W. ; BATCHELOR, Andrew W.: *Engineering Tribology*. 4. Aufl. Oxford, UK : Butterworth-Heinemann, 2014

[16] PERSSON, B.N.J.: *Contact mechanics for randomly rough surfaces*. In: *Surface Science Reports* 61 (2006), Nr. 4, S. 201–227

[17] HOFMEISTER, Marius ; FISCHER, Felix ; BODEN, Lukas ; SCHMITZ, Katharina: Simulative Prediction of Leakage for Seat Valves and Bio-Hybrid Fuels. In: *22nd International Sealing Conference 2024, Stuttgart, Germany*, S. 141–154

[18] GREENWOOD, J. A. ; WILLIAMSON, J. B. P.: *Contact of nominally flat surfaces*. In: *Proceedings of the Royal Society of London. Series A. Mathematical and Physical Sciences* 295 (1966), Nr. 1442, S. 300–319

[19] BELL, Ian H. ; WRONSKI, Jorrit ; QUOILIN, Sylvain ; LEMORT, Vincent: *Pure and Pseudo-pure Fluid Thermophysical Property Evaluation and the Open-Source Thermophysical Property Library CoolProp*. In: *Industrial & Engineering Chemistry Research* 53 (2014), Nr. 6, S. 2498–2508

[20] SHARP, Kendra V. ; ADRIAN, Ronald J. ; SANTIAGO, Juan G. ; MOLHO, Joshua I.: *The MEMS Handbook: Liquid Flow in MIcrochannels* : CRC Press LLC, 2002

9 Authors

RWTH Aachen University, Institute for Fluid Power Drives and Systems (ifas)
Campus-Boulevard 30, 52074 Aachen, Germany:

Marius Hofmeister, M. Sc., ORCID 0000-0002-6672-5800,
marius.hofmeister@ifas.rwth-aachen.de

Anmol Kasera, M. Sc., ORCID 0009-0007-4004-7670,
anmol.kasera@ifas.rwth-aachen.de

Georg Michael Puntigam, M. Sc., ORCID 0009-0009-9472-6323,
georg.puntigam@ifas.rwth-aachen.de

Felix Justin Fischer, M. Sc., ORCID 0000-0003-2081-1823,
f.fischer@ifas.rwth-aachen.de

Univ.-Prof. Dr.-Ing. Katharina Schmitz, ORCID 0000-0002-1454-8267,
katharina.schmitz@ifas.rwth-aachen.de